UDC 553.41

A. V. SNACHEV[1], *Head of Laboratory, Candidate of Geological and Mineralogical Sciences, SAVant@rambler.ru*
A. V. PANTELEEVA[1], *Researcher, Candidate of Geological and Mineralogical Sciences*
M. A. RASSOMAHIN[2], *Junior Researcher*

[1]*Institute of Geology, Ufa Federal Research Center, Russian Academy of Sciences, Ufa, Russia*
[2]*South Ural Federal Research Center for Mineralogy and Geoecology, Ural Branch, Russian Academy of Sciences, Miass, Russia*

RARE-EARTH MINERALS IN CARBONACEOUS SHALE OF THE KUMAK GOLD DEPOSIT, SOUTH URALS, RUSSIA

The article presents the results of the study of carbonaceous shales from the Kumak deposit. The analysis of their geochemical features reveals their shallow water–near shore sedimentation conditions. The high-aluminous terrigenous sedimentary material underwent minimal transport and was formed mainly due to destruction of basic rocks. The sediments experienced a high degree of weathering typical of humid climates and deposited under conditions of oxidation and pre-oxidation.

It is found that rare-earth elements (REE) practically do not accumulate in carbonaceous shales; their contents are correlated directly with the amount of terrigenous admixture, Normalization with respect to Post-Archean Australian shales (PAAS) shows that REE contents are in the range from 0.1 to 1 units. The carbonaceous shales are characterized by uniform normalized curves–preferential accumulation of light REE as against heavy REE, with a distinct europium minimum in a number of samples.

The main minerals-concentrators for light REE are Monazite-(Ce) and Rhabdophane-(Ce), and for heavy REE–Xenotime-(Y). Xenotime is an yttrium mineral, with the content of Y_2O_3 up to 47.61 wt.%. Among the other REE which regularly replace yttrium, dysprosium, gadolinium and erbium prevail. Monazite is a cerium mineral, with the content of Ce_2O_3 up to 37.07 wt.%. The ratio of Ce_2O_3 to the sum of the other light REEs is stable and equals 1. In contrast to xenotime, monazite contains a significant thorium admixture reaching 13.32 wt.% of ThO_2. Georceixite, bastnasite and pietersite-(Ce), which is an agardite-(Ce) mineral, are represented by single grains. A large number of Th–REE compounds of complex composition and an unidentified As-Ce mineral in zircon are also observed.

Keywords: *Southern Urals, Kumak ore field, carbonaceous shales, black shales, rare-earth minerals, gold, xenotime-(Y), monazite-(Ce), rhabdophane-(Ce)*
DOI: *10.17580/em.2023.02.01*

Introduction

Geologists have a steadily high interest in carbonaceous shales as this is a favorable geochemical environment for the primary accumulation of many minerals, including ore, containing rare earths. In tectonically and magmatically active zones, carbonaceous shales can be both a source of ore-bearing fluids and a host of large gold ore deposits (Sukhoi Log, Muruntau, Kumtor, Natalka, Svetly and other) [1–10]. The Kumak ore field has been an object of comprehensive research by the Central Research Geological Exploration Institute of Non-Ferrous and Noble Metals since 1960 (researchers N. M. Voin, Yu. A. Burmin, N. I. Borodaevsky and other). Some investigators studied the structure of the deposit, gold mineralization patterns and material constitution [11–14]. The geomechanical peculiarities of the ore-hosting black shale, carbon matter and rare-earth mineralization were neglected.

Research methods

The geochemistry of carbonaceous shales was studied using the microanalysis by ICP-MS spectrometry on analyzers ELAN 900 and Nex-ION300, with the classification into rare earths (14 REE) and trace elements (26 elements of Li, B, Be, Sc, Ti, Cr, Ni, V, Co, Cu, Zn, Ga, Rb, Sr, Y, Zr, Nb, Mo, Sb, Cs, Ba, Hf, Ta, Pb, Th, U) (Academician Zavaritsky Institute of Geology and Geochemistry, UB RAS, Yekaterinburg).

The chemical composition was determined using SEM Tescan Vega 3 with energy-dispersive spectrometer Oxford Instruments X-act at the Sharing Center of the Southern-Ural Federal Research Center for Mineralogy and Geoecology, UB RAS (analyst M. A. Rassomakhin, carbon coating, boosting voltage of 20 kV, "live" time of 120 s, basic reference standards—Microanalysis consultants LTD, UN1362). Direct test objects were microsections.

Geological structure

The Kumak ore field occurs at the coupling zone of the Anikhovka deep faulting and the through systems of near-latitudinal and diagonal dislocations (Orsk Belt and Kempisarai Belt, respectively). The Anikhovka fault trough is mostly composed of Bereznyaki basalt–andesite–rhyolite extrusive rocks (D_3-C_1bz) and Breda carbonaceous terrigenous–carbonate shales (C_1bd) [15] (**Fig. 1**). The volcanic sedimentary rocks are cut with numerous intrusive rocks from the Dzhabygasai diorite–plagiogranite–gabbro ($p\gamma$-$\gamma\delta$-νD_3d) and Kumak diorite–plagiogranite (δC_1k) systems [13, 17, 18].

The main commercial-value object in the ore field is the Kumak gold deposit. Geologically, it is inseparable from the Low-Carbon carbonaceous–graphitic shales and adjoins the center of the syncline. Gold mineralization concentrates in the narrow and steeply dipping zones of subalcalic metasomatic rocks which intersect sedimentary strata and represent mostly sericite–quartz and quartz–chlorite–sericite shales with tourmaline (see fig. 1). The metasomatic rocks extend for round 4.5 km at the thickness to 120 m, and the average gold content of the deposit is 7–10 g/t. The prime value is the sheet-like and lens-like ore bodies accompanied with the zones of silicification and sulfidation, and passing into foliated and altered quartz diorite at depth.

The Kumak ore is dominated by fine high-karat gold (Au 90–96%) associated with gold–bismuth–telluride and native gold–tourmaline assemblages [18]. The oxidation zone contains a little of supergene gold at an average amount of 2% of total gold. At the ore outcrops at ground surface, there are many traces of free digging at eluvial–deluvial placers, and mined-out underground openings and dug holes in oxidized ledge ore down to the depths of 10–25 m. In the north, there is a thick (to 20 m) clayey overburden above the ore outcrops.

Geochemical peculiarities of carbonaceous shales

The ore-enclosing strata in the Kumak field represent mostly carbon-bearing siltstone and carbonaceous–clayey shale. The elemental composition features the increased contents of MgO (0.60–6.42%), TiO_2 (0.29–1.89%) and Al_2O_3 (9.40–31.50%), and, accordingly, the increased hydrolyzate module (>0.55 units) and alumosilicic module (0.77 units, average 0.38 units). Lithochemically, they conform with siallite and super aluminum hydrolyzate rocks associated with residuum and including high percentage of volcanogenic material [19]. High-repeatability chemical indexes of alteration (CIA = $100Al_2O_3$ / (Al_2O_3 +

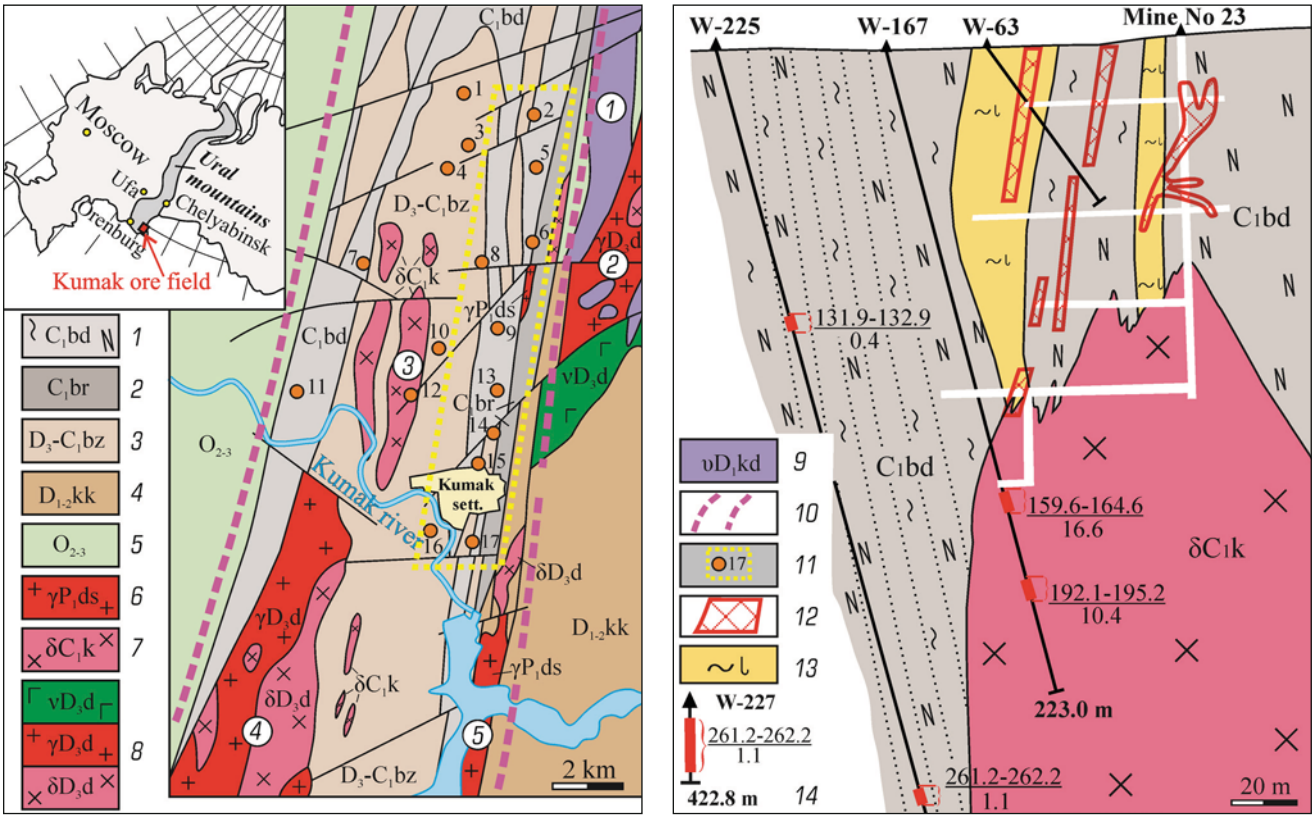

Fig. 1. Geological map of Kumak ore field, and a standard cross-section with gold assaying data (according to P.V. Lyadovsky [16] and from appraisal surveys accomplished by E.E. Mironov and M.I, Novgorodova in 1974–1979)

Legend:

1 – Breda series (carbonaceous shale, sandstone, siltstone); *2* – Birgilda strata (conglomerates, sandstone, limestone); *3* – Bereznyaki strata (basic and acid tuff, siltstone interlayers); *4* – Kokpekty strata (lavas and basaltic tuff); *5* – Ordovician volcano–sedimentary strata, undifferentiated; *6* – Dzhabyk–Sanary granite–leucogranite complex; *7* – Kumak diorite–plagiogranite complex; *8* – Dzhabygasai diorite–plagiogranite–gabbro complex; *9* – Kamenny Dol ultra mafite complex; *10* – boundary of Anikhovka fault trough; *11* – boundary of Kumak ore field and gold deposits: *1* – Caesar, *2* – Yermak, *3* – Tanin, *4* – Vasin, *5* – East Tykasha, *6* – Kommercheskoe, *7* – Tamara, *8* – Milya, *9* – Transbaikal, *10* – Amur, *11* – Predator, *12* – Proliv, *13* – Baikal, *14* – Central, *15* – Kumak, *16* – Zarechnoe, *17* – Southern Kumak; *12* – ore body outlines; *13* – ore-bearing quartz–mica–tourmaline metasomatic rocks in carbonaceous shales; *14* – wells, lengths, sampling intervals and gold contents (g/t). Intrusive rock mass (circled figures): *1* – Kairakty, *2* – Dzhabygasai, *3* – Tykasha, *4* – Akzhar, *5* – Kumak dike

Table 1. Contents of rare earths and trace elements in carbonaceous shales in Kumak ore field (ppm)

	KM015g	KM024g	KM005s	KM031s	KM044s	KM032s
La	6	22	17	8	6	9
Ce	15	42	33	17	17	24
Pr	1.8	6.3	3.8	2	2.2	2.8
Nd	7	27	15	8	10	12
Sm	1.4	6.0	2.8	1.6	2.4	2.5
Eu	0.5	0.9	0.7	0.5	0.5	0.6
Gd	1.2	4.0	3.2	1.3	2.1	2.0
Tb	0.14	0.50	0.50	0.16	0.28	0.24
Dy	0.7	2.2	2.9	0.8	1.6	1.4
Ho	0.12	0.40	0.60	0.15	0.30	0.26
Er	0.36	1.10	1.60	0.45	0.90	0.70
Tm	0.06	0.16	0.22	0.07	0.13	0.11
Yb	0.4	1.0	1.4	0.5	0.9	0.8
Lu	0.07	0.16	0.21	0.08	0.16	0.13
Y	2	10	16	4	5	5
∑ REE	34.74	113.72	82.93	40.60	44.47	56.54
Note: KM015g — sample number						

+ CaO + Na_2O + K_2O)) [20], from 70 to 94 units, and the ratio log(SiO_2/Al_2O_3)–log(Fe_2O_{3total}/K_2O) [21] point at the high-scale alteration of sedimentary aluminosilicate clastic material, typical of humid zones, and at minimum transport. The patterns of the imaging points of the carbonaceous shale composition in the diagrams La/Sc–Th/Co [22] and F1-F2 [23] show that the source of the terrigenous material is predominantly the basic rocks and the washout product of acid volcanic rocks at the bottom of the Breda cross-section. Considering the high content of terrigenous impurities, the minimum transport of the sedimentary material and the presence of limestone interbeds in the cross-sections, dominated by micro fauna, the test shales can be characterized as the shallow-water–near shore deposits.

By totality of values of V/Cr, V/(V+Ni), Mo/Mn, U_a=U_{total}–Th/3 [24, 25], the Breda carbonaceous sedimentary rocks deposited in oxidative and partly suboxidative environment. The chalcophile elements, such as copper, zinc and lead, are present in black shales of the Kumak ore field in small amounts (first tens of ppm). At the bottom of the ore-bearing zones adjoined to the apical systems in quartz diorite strata, the increased contents of Mo, Co, W, Cu and Nb are observed. The superimposed hydrothermal areas match with the high-contrast anomalies of As, Ag, as well as Cu, Pb, Zn, B, Bi, Ni and Co. The average contents of arsenic gradually grow south-northwards of the ore field, and are maximal (0.1%) in the mineralized zone of the Yermak site (see fig. 1).

The rare earths undergo almost no accumulation in carbonaceous shales of the Kumak field, and the normalized contents of most rare earths get in the interval from 0.1 to 0.3 units (**Fig. 2*a*, Table 1**). The sum of REE is

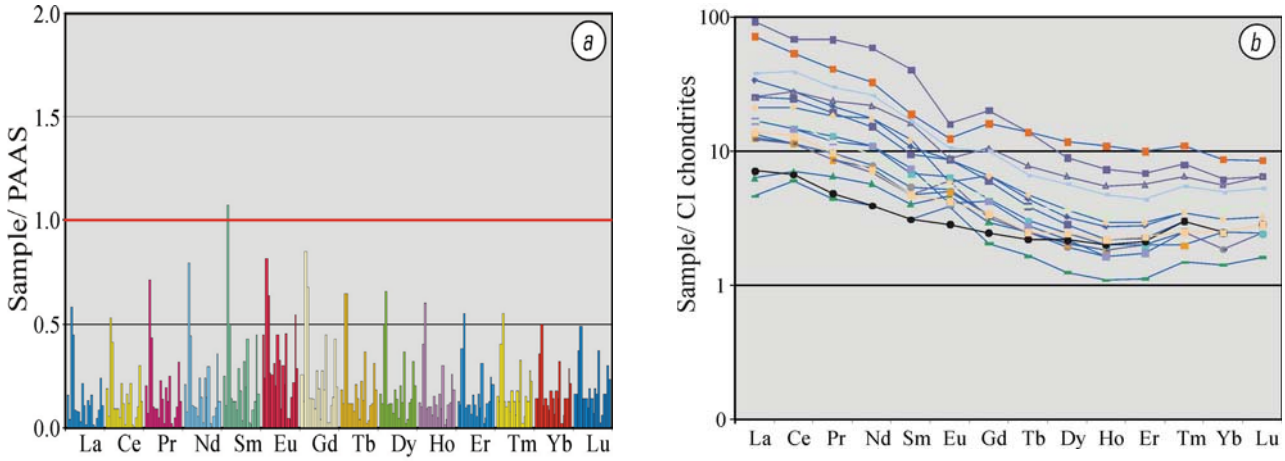

Fig. 2. Normalization of rare earth contents in Kumak carbonaceous shales with respect to Post-Archean Australian shales (PAAS) [26] (*a*) and to chondrite CI [27] (*b*)

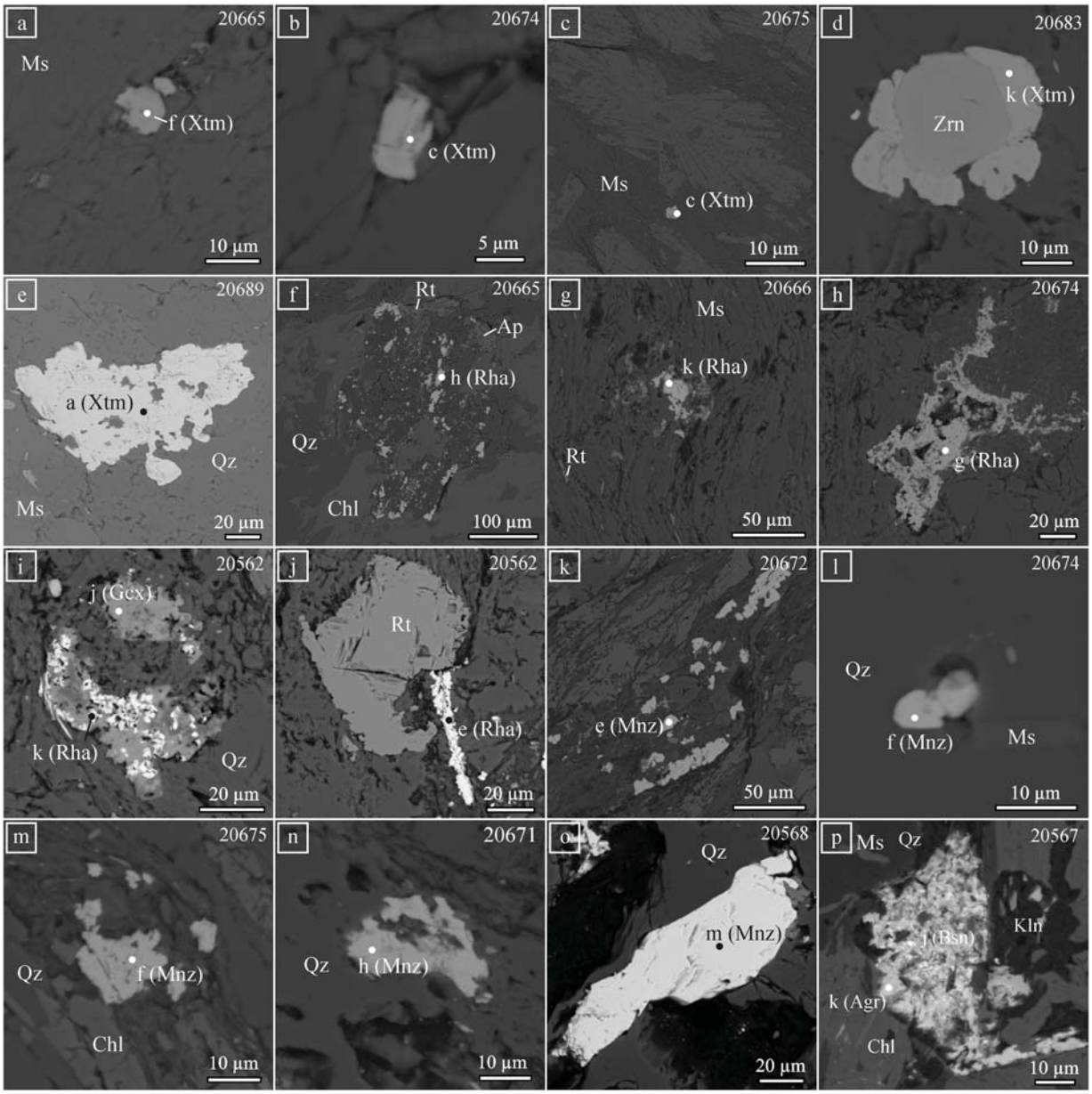

Fig. 3. Rare-earth minerals in Kumak carbonaceous shales

Legend: Mineral symbols as per [33]: Agr–Agardite, Ap–Apatite, Bsn–Bastnäsite, Chl–Chlorite, Gcx–Gorceixite, Kln–Kaolinite, Mnz–Monazite-(Ce), Ms–Muscovite, Qz–Quartz, Rha–Rhabdophane-(Ce), Rt–Rutile, Xtm–Xenotime-(Y), Zrn–Zircon

Table 2. Chemical composition of Xenotime-(Y) from Kumak carbonaceous shales

Analysis	SiO_2	P_2O_5	CaO	FeO	Y_2O_3	Sm_2O_3	Gd_2O_3	Tb_2O_3	Dy_2O_3	Ho_2O_3	Er_2O_3	Yb_2O_3	ThO_2	UO_2	Total
21722c	2.06	33.84			39.83	1.36	11.49		5.07		3.47	2.99		0.74	100.88
21722h	1.45	34.14			47.61	0.23	3.54		4.96	1.44	3.61	3.19		0.56	100.74
21722o	1.92	33.10			44.40		6.20		4.98		3.55	3.91	0.36	0.52	98.92
20665f		35.43		1.87	46.27		3.08		3.67		4.26	6.24			100.82
20671c		34.79			43.53		8.38		5.21		3.56	3.61	0.17	0.45	99.70
20674c		34.20			40.35		14.73	1.44	5.86		2.15	1.28			100.00
20675c		35.91			46.25		5.90		4.82		3.69	3.03			99.60
20683k	1.71	33.42	0.18		44.41		7.66		5.86		2.98	2.16		0.81	99.19
20689a		34.14			44.48		7.28		4.99		3.86	4.71			99.46
Analysis	**Formula**														
21722c	$Y_{0.71}Gd_{0.13}Dy_{0.05}Er_{0.04}Yb_{0.03}Sm_{0.02}U_{0.01}P_{0.96}Si_{0.07}O_4$														
21722h	$Y_{0.83}Dy_{0.05}Gd_{0.04}Er_{0.04}Yb_{0.03}Ho_{0.01}Sm_{0.002}P_{0.94}Si_{0.05}O_4$														
21722o	$Y_{0.79}Gd_{0.07}Dy_{0.05}Er_{0.04}Yb_{0.04}U_{0.004}Th_{0.003}P_{0.94}Si_{0.06}O_4$														
20665f	$Y_{0.80}Yb_{0.06}Fe_{0.05}Dy_{0.04}Er_{0.04}Gd_{0.03}P_{0.97}O_4$														
20671c	$Y_{0.78}Gd_{0.09}Dy_{0.06}Er_{0.04}Yb_{0.04}U_{0.003}Th_{0.001}P_{0.99}O_4$														
20674c	$Y_{0.73}Gd_{0.17}Dy_{0.06}Er_{0.02}Tb_{0.01}Yb_{0.01}P_{0.99}O_4$														
20675c	$Y_{0.81}Gd_{0.06}Dy_{0.05}Er_{0.04}Yb_{0.03}P_{1.00}O_4$														
20683k	$Y_{0.79}Gd_{0.08}Dy_{0.06}Er_{0.03}Yb_{0.02}Ca_{0.01}U_{0.006}P_{0.94}Si_{0.06}O_4$														
20689a	$Y_{0.80}Gd_{0.08}Yb_{0.05}Dy_{0.05}Er_{0.04}P_{0.98}O_4$														

Table 3. Chemical composition of Monazite-(Ce) from Kumak carbonaceous shales

Analysis	SiO_2	P_2O_5	CaO	La_2O_3	Ce_2O_3	Pr_2O_3	Nd_2O_3	Sm_2O_3	Gd_2O_3	Dy_2O_3	ThO_2	UO_2	Total
20671h	0.82	29.38	1.38	13.50	29.87	2.86	10.88	1.32			8.52	0.57	99.10
20672e	0.27	28.93	0.37	11.71	32.70	3.54	14.68	3.19	4.03				99.41
20672f	1.28	26.37	1.04	11.51	30.69	3.40	12.54	2.23	2.43	0.47	3.28	0.05	95.29
20673c	0.83	28.75	1.18	16.14	29.71	2.65	10.48	1.09			8.77		99.59
20674f	0.94	29.11		11.64	37.07	3.51	12.83	1.94	1.89		0.63	0.18	99.73
20675f	1.28	27.50	1.20	14.69	32.43	3.18	11.78	1.14	2.01		2.63		97.84
20683j	3.40	23.58	0.62	18.74	29.11		6.52				13.32		95.29
20568m		30.41	0.55	15.45	31.23	3.48	12.52	2.33	1.52		1.45	0.20	99.14
Analysis	**Formula**												
20671h	$Ce_{0.43}La_{0.20}Nd_{0.15}Th_{0.08}Ca_{0.06}Pr_{0.04}Sm_{0.02}U_{0.005}P_{0.98}Si_{0.03}O_4$												
20672e	$Ce_{0.47}Nd_{0.21}La_{0.17}Gd_{0.05}Pr_{0.04}Sm_{0.04}Ca_{0.02}P_{0.97}Si_{0.01}O_4$												
20672f	$Ce_{0.46}Nd_{0.19}La_{0.18}Ca_{0.05}Pr_{0.05}Sm_{0.03}Gd_{0.03}Th_{0.03}Dy_{0.01}U_{0.005}P_{0.92}Si_{0.05}O_4$												
20673c	$Ce_{0.43}La_{0.24}Nd_{0.15}Th_{0.08}Ca_{0.05}Pr_{0.04}Sm_{0.01}P_{0.97}Si_{0.03}O_4$												
20674f	$Ce_{0.53}Nd_{0.18}La_{0.17}Pr_{0.05}Sm_{0.03}Gd_{0.02}Th_{0.01}U_{0.002}P_{0.97}Si_{0.04}O_4$												
20675f	$Ce_{0.47}La_{0.22}Nd_{0.17}Ca_{0.05}Pr_{0.05}Gd_{0.03}Sm_{0.02}Th_{0.02}P_{0.93}Si_{0.05}O_4$												
20683j	$Ce_{0.45}La_{0.29}Th_{0.13}Nd_{0.10}Ca_{0.03}P_{0.85}Si_{0.14}O_4$												
20568m	$Ce_{0.45}La_{0.22}Nd_{0.18}Pr_{0.05}Sm_{0.03}Gd_{0.02}Ca_{0.02}Th_{0.01}U_{0.002}P_{1.01}O_4$												

Table 4. Chemical composition of Rhabdophane-(Ce) from Kumak carbonaceous shales

Analysis	Al_2O_3	SiO_2	P_2O_5	CaO	FeO	SrO	La_2O_3	Ce_2O_3	Pr_2O_3	Nd_2O_3	Sm_2O_3	Gd_2O_3	ThO_2	Total
20665h		1.15	28.88	1.09		0.77	13.80	29.15		12.22	1.53	3.40	1.25	93.25
20666k			28.94	0.44			15.30	33.07	3.51	12.64	1.03		1.64	96.56
20562e	0.71	0.88	26.79	1.06	0.37		12.95	34.21	3.22	11.38	1.35	3.40		96.33
Analysis	**Formula**													
20665h	$Ce_{0.43}La_{0.21}Nd_{0.18}Gd_{0.05}Ca_{0.05}Sm_{0.02}Sr_{0.02}Th_{0.01}P_{0.99}Si_{0.05}O_4$													
20666k	$Ce_{0.49}La_{0.23}Nd_{0.18}Pr_{0.05}Ca_{0.02}Sm_{0.01}Th_{0.02}P_{1.00}O_4$													
20562e	$Ce_{0.50}La_{0.19}Nd_{0.16}Gd_{0.05}Ca_{0.05}Sm_{0.02}Fe_{0.01}P_{0.91}Si_{0.04}Al_{0.03}O_4$													

directly correlated with the quantity of terrigenous substance in the sedimentation basin (hydrolyzate and alumosilicic moduli) and finds room within the interval of 30–50 ppm, and seldom reaches 100 ppm (see Table 1, sample KM024g).

Normalizing applied to CI chondrite (**Fig. 2*b***) revealed a certain regular pattern in the contents of rare earths (in this study, normalizing of chondrite used the data of H. Wakita et al. [27]). The Breda carbonaceous shale strata feature uniform normalized curves—predominate accumulation of light rather than heavy REE, with a distinct europium minimum in some samples (see fig. 2*b*). Furthermore, there is a steady correlation between the light REE (La:Ce:Nd is 1:2:1) (see Table 1), which is typical of the majority of carbonaceous shales [28–32].

Rare-earth minerals in carbonaceous shales

The authors have revealed rare earths in carbonaceous shales of the Kumak field. The main minerals–concentrators are monazite-(Ce) and rhabdophane-(Ce) for the light rare earths, and xenotime-(Y) for the heavy rare earths (**Fig. 3**). Georceixite, bastnasite and pietersite-(Ce), which is a agardite-(Ce) mineral, are present as single grains, and there is also much quantity of complex-composition Th–REE compounds, and an unidentified As-Ce mineral in zircon.

The most widespread is *xenotime-(Y)* represented by mostly fine (to 10 μm) and irregular-shape grains which fill the voids in the quartz–muscovite matrix (see fig. 3*a*, *b*) and are present on zircon crystals as syntactic nodes (see fig. 3*d*). Xenotime is an yttrium mineral with the contents of Y_2O_3 from 39.83 to 47.61 wt.% and Yb_2O_3 from 1.28 to 6.24 wt.%. The other rare earths which replace yttrium in the composition of xenotime are dysprosium (Dy_2O_3—3.67–5.86 wt.%), gadolinium (Gd_2O_3—3.08–14.73 wt.%) and erbium (Er_2O_3—2.15–4.26 wt.%). Admixtures of ThO_2 and UO_2 are insignificant and total to not more than 1 wt. % (**Table 2**).

Monazite-(Ce) occurs as whole and fragmented applanate grains 50–100 μm in size between carbonaceous–micaceous interlayers (see fig. 3k, o), or as fine (to 20 μm) grains of irregular shape in the micro voids between the quartz and muscovite grains (see fig. 3. l, m, n). Monazite is a cerium mineral with the content of Ce_2O_3 from 29.11 to 37.07 wt.%. The ratio of Ce_2O_3 to the sum of the rest light rare-earth oxides ($La_2O_3+Pr_2O_3+Nd_2O_3+Sm_2O_3$) is stable and equals 1. As against xenotime, monazite contains a substantial admixture of thorium at 13.32 wt.% (**Table 3**).

Rhabdophane-(Ce) is present in concretion with rutile and apatite in the form of irregular-shape aggregates 20–100 μm in size, and as a result of secondary replacement of monazite-(Ce) with the preserved admixture elements in its composition (**Table 4**).

Considering the stable inverse relation between the content of CaO and the sum of the rare earths in monazite and rhabdophane, it can be supposed that some rare earths appeared in carbonaceous shales as a result of exocontact influence of Kumak diorites [34].

Conclusions

From the geochemical and mineralogical analysis of carbonaceous strata in the Kumak field, it is possible to draw some conclusions which are listed below.

1. By the set of parameters ($\log(SiO_2/Al_2O_3)$–$\log(Fe_2O_{3total}/K_2O)$; La/Sc–Th/Co; F1-F2) and from the presence of limestone interbeds dominated by micro fauna in the cross-sections, the conditions of sedimentation can be characterized as shallow water–near-shore, with mostly terrigenous source of drifting. Highly aluminous sedimentary material underwent minimum transport, and formed mostly owing to destruction of Breda-series basic and acid volcanic rocks.

2. The steadily high values of the index of chemical alteration (CIA) are typical of the moist hymide climate. The ratios of V/Cr, V/(V+Ni), Mo/Mn, $U_a=U_{total}$–Th/3 are indicative of oxidative and partly sub-oxidative environment of sedimentation.

3. Rare earths experience almost no accumulation in carbonaceous shales, and normalization with respect to Post-Archean Australian shales (PAAS) shows that the contents of REE fit in the interval from 0.1 to 1 units. Considering the direct correlation between the sum of REE and hydrolyzate and alumosilicic moduli, we think that REE appeared in the sedimentation basin with the terrigenous admixture.

4. The carbonaceous shales are characterized with the uniform normalized curves—light REE dominate over heavy REE. The main minerals–concentrators are monazite-(Ce) and rhabdophane-(Ce) for the light REE, and xenotime-(Y) for the heavy REE.

Acknowledgement

The study was supported by the Russian Science Foundation, Grant No. 23-27-00265, https://rscf.ru/en/project/23-27-00265/.

References

1. Arifulov Ch. Kh. Black shales gold deposits of various geological conditions. *Rudy i Metally*. 2005. No. 2. pp. 9–19.
2. Gadd M. G., Peter J. M., Jackson S. E., Zhaoping Yang, Petts D. Platinum, Pd, Mo, Au and Re deportment in hyper-enriched black shale Ni-Zn-Mo-PGE mineralization, Peel River, Yukon, Canada. *Ore Geology Reviews*. 2019. Vol. 107. pp. 600–614.
3. Groves D. I., Goldfarb R. J., Robert F., Hart C. J. R. Gold deposits in metamorphic belts: Overview of current understanding, outstanding problems, future research, and exploration significance. *Economic Geology*. 2003. Vol. 98, No. 1. pp. 1–29.
4. Ivanov A. I. The role played by metamorphic transformation conditions of carbonaceous carbonate–terrigenous deposits for gold mineralization formation at various stages of collisional epoch of Baikal-patom metallogenic province development. *Otechestvennaya geologiya*. 2017. No. 4. pp. 3–23.
5. Ketris M. P., Yudovich Ya. E. Estimation of clarkes for carbonaceous biolithes: World averages for trace elements contents in black shales and coals. *International Journal of Coal Geology*. 2009. Vol. 78, No. 2. pp. 135–148.
6. Large R. R., Bull S. W., Maslennikov V. V. A carbonaceous sedimentary source-rock model for Carlin type and orogenic gold deposits. *Economic Geology*. 2011. Vol. 106, No. 3. pp. 331–358.
7. Shumilova T. G., Shevchuk S. S., Isayenko S. I. Metal concentrations and carbonaceous matter in the black shale type rocks of the Urals. *Doklady Earth Sciences*. 2016. Vol. 469, No. 1. pp. 695–698.
8. Snachev A. V., Puchkov V. N. First findings of palladium–gold–REE ore mineralization in Precambrian carbonaceous shales on the western slope of the Southern Urals. *Doklady Earth Sciences*. 2010. Vol. 433, No. 1. pp. 866–869.
9. Vysotsky S. I., Kovalev S. G. Geochemistry of rare-earth elements and noble metals in rock of the Shatak complex (South Urals). *Geologicheskii vestnik*. 2019. No. 2. pp. 58–71.
10. Xu L., Lehmann B., Mao J. Seawater contribution to polymetallic Ni-Mo-PGE-Au mineralization in Early Cambrian black shales of South China: Evidence from Mo isotope, PGE, trace element, and REE geochemistry. *Ore Geology Reviews*. 2013. Vol. 52. pp. 66–84.
11. Albov M. N. Secondary zoning of gold deposits in the Urals. Moscow : Gosgeoltekhizdat, 1960. 215 p.
12. Bilibina T. V., Bogdanov Yu. V. On the prospects of gold potential in the Mugodzhar region. *Geologiya rudnykh mestorozhdeniy*. 1959. No. 5. pp. 104–111.
13. Sazonov V. N., Koroteev V. A., Ogorodnikov V. N., Polenov Yu. A., Velikanov A. Ya. Gold in "black shales" of the Urals. *Litosfera*. 2011. No. 4. pp. 70–92.
14. Voin M. I. Features of structure and mineralization in the Kumak ore field and the detection procedure of rich pay zones in crushed veins. *Izvestiya vuzov. Geologiya i razvedka*. 1966. No. 11. pp. 77–86.
15. Kolomoets A. V., Snachev A. V. Geology and petrogeochemical features of the Kumak ore field carbonaceous shales. *Processes in GeoMedia*. 2021. Vol. 3. pp. 25–35.

16. Lyadskiy P. V., Chen-Len-Son B. I., Kvasnyuk L. N., Alekseeva G. A., Olenitsa T. V. et al. State geological map of the Russian Federation. Scale 1:200 000. 2nd Edition. Series South Ural. Sheet M-41-VII(XIII) (Svetly). Explanatory note. Moscow MF FGBU VSEGEI, 2018. 128 p.
17. Kolomoets A. V., Snachev A. V., Rassomakhin M. A. Gold–tourmaline mineralization in carbonaceous shales of the Kumak deposit (South Ural). *Gornyi Zhurnal*. 2020. No. 12. pp. 11–15.
18. Snachev A. V., Kolomoets A. V., Rassomakhin M. A., Snachev V. I. Geology and gold content of carbonaceous shale in Baikal mineralization site, Southern Ural. *Eurasian Mining*. 2021. No. 1. pp. 8–13.
19. Yudovich Ya. E., Ketris M. P. Geochemistry of black shales. Moscow. Berlin: Direct Media, 2015. 272 p.
20. Nesbitt H. W., Young G. M. Early Proterozoic climates and plate motions inferred from major element chemistry of lutites. *Nature*. 1982. Vol. 299. pp. 715–717.
21. Herron M. M. Geochemical classification of terrigenous sands and shales from core or log data. *Journal of Sedimentary Petrology*. 1988. Vol. 58. pp. 820–829.
22. Cullers R. L. Implications of elemental concentrations for provenance, redox conditions, and metamorphic studies of shales and limestones near Pueblo, CO, USA. *Chemical Geology*. 2002. Vol. 191, No. 4. pp. 305–327.
23. Roser B. P., Korsch R. J. Provenance signatures of sandstone–mudstone suites determined using discriminant function analysis of major-element data. *Chemical Geology*. 1988. Vol. 67, Iss. 1–2. pp. 119–139.
24. Jones B., Manning D. Comparison of geochemical indices used for the interpretation of paleoredox conditions in ancient mudstones. *Chemical Geology*. 1994. Vol. 111, Iss. 1–4. pp. 111–129.
25. Kholodov V. N., Naumov R. I. On the geochemical criteria for the appearance of hydrogen sulfide contamination in the waters of ancient reservoirs. *Proceedings of the Academy of Sciences of the USSR. Geology series*. 1991. Vol. 12. pp. 74–82.
26. Taylor S. R., Mc Lennan S. M. The Continental Crust: Its Composition and Evolution. Blackwell : Oxford, UK, 1985. 312 p.
27. Wakita H., Rey P., Schmitt R. A. Abundances of the 14 rare-earth elements and 12 other trace elements in Apollo 12 samples: fife igneous and one breccia rocks and four soils. *Proceedings of the 2nd Lunar Science Conference*. Oxford : Pergamon Press. 1971. pp. 1319–1329.
28. Cherepanov A. A., Berdnikov N. V., Shtareva A. V. Rare-earth elements and noble metals in phosphorites of the Gremuchy Occurrence, Lesser Khingan, Far East of Russia. *Russian Journal of Pacific Geology*. 2019. Vol. 13, No. 6. pp. 585–593.
29. Cherepanov A. A., Berdnikov N. V., Shtareva A. V., Krutikova V. O. Formation conditions and rare-earth mineralization of Riphean Carbonaceous shales of the Upper Nyatygran subformation, Russian Far East. *Russian Journal of Pacific Geology*. 2017. Vol. 11, No. 4. pp. 297–307.
30. Paikaray S., Banerjee S., Mukherji S. Geochemistry of shales from the Paleoproterozoic to Neoproterozoic Vindhyan Supergroup: Implications on provenance, tectonics and paleoweathering. *Journal of Asian Earth Sciences*. 2008. Vol. 32, Iss. 1. pp. 34–48.
31. Palenova E. E., Rozhkova E. A., Belogub E. V., Rassomakhin M. A. MREE minerals in black shales of the Paleoproterozoic Mikhailovka formation (Baikal-Patom highland, Siberia). *Mineralogy*. 2022. Vol. 8, No. 3. pp. 47–66.
32. Zanin Yu. N., Zamirailova A. G., Eder V. G., Krasavchikov V. O. Rare-earth elements in the Bazhenov formation of the West-Siberian sedimentary basin. *Lithosphere*. 2011. No. 6. pp. 38–54.
33. Warr L. IMA–CNMNC approved mineral symbols. *Mineralogical Magazine*. 2021. Vol. 85, Iss. 3. pp. 291–320.
34. Kovalev S. G., Maslov A. V., Kovalev S. S. Mineralogical and geochemical aspects of rare-earth elements behavior during metamorphism (on the example of the Upper Precambrian structural-material complexes of the Bashkir megaanticlinorium, South Urals). *Georesources*. 2020. Vol. 22, No. 2. pp. 56–66. EM

UDC 550.8:550.4:550.3

I. M. A. ELSHARIF[1], *Post-Graduate Student, mohammedelsharif7@gmail.com*
A. G. KOTELNIKOV[1], *Associate Professor, Head of Department, Candidate of Geological and Mineralogical Sciences*
A. F. GEORGIEVSKIY[1], *Associate Professor, Doctor of Geological and Mineralogical Sciences*
S. A. IBRAHIM[2], *Head of Department, Candidate of Geological and Mineralogical Sciences*

[1]*Peoples' Friendship University of Russia (RUDN University), Moscow, Russia*
[2]*University of Khartoum, Khartoum, Sudan*

GEOCHEMISTRY AND PETROGENESIS OF SYROSTAN GRANITOID INTRUSIONS IN THE SOUTHERN URALS

Introduction

Granite intrusions are often associated with different minerals (for example, ores W, Sn, Nb, Ta, Li, Be, Rb, Cs and REE) [1, 2]. There are some known ore runs within the Syrostan Massif, including skarn bodies and gold-bearing quartz veins. Understanding of distribution of elements in the course of their evolution from magma to hydrothermal phase indispensably requires a profound knowledge on petrogenesis and tectonic mechanism of granite intrusions.

This study aims to reveal petrological features of the Syrostan granite to improve understanding of its formation conditions and mineralization potential.

The article characterizes geochemistry and petrogenesis of granitoids of the Syrostan Massif located southwest of the town of Miass, in the zone of the main deep fault in the Urals. The geochemistry of the collected samples from Syrostan was analyzed using ICP-MS and the X-ray fluorescence. Granite is rich in silicon oxide SiO_2 at its concentrations from 59.54 to 76.14 wt.%. The rocks are from metaluminous to peraluminous and belong to the high-K calc-alkaline to weakly calc-alkaline series; granite is type I and has A/CNK < 1. The test samples feature the higher content of LREE as compared with HREE, the ratios (La / Sm)N from 3.5 to 6.5 and (Gd /Yb)N from 1.25 to 2.8, and the negative Eu anomaly. The revealed negative Nb anomalies and the ratio Nb/Ta (8–16) <17 point at depletion of mantle melts. These results can be reflective of the granite formation in the tectonic environment of the volcanic arc. Understanding of the petrogenesis of granitoids in the Syrostan Massif can help predict commercial accumulations of rare metals in it.

Keywords: *Syrostan Massif, geochemistry, high alkaline granites, type I granite, continental crust, depleted mantle, volcanic arc, ICP-MS*
DOI: *10.17580/em.2023.02.02*